Inverse Design of Supersonic Airfoils Using Integral Equations

Shinkyu Jeong*
Tohoku University, Sendai 980-8579, Japan
Kisa Matsushima†
Fujitsu Laboratories Ltd., Chiba 261, Japan
Toshiyuki Iwamiya‡
National Aerospace Laboratory, Chofu, Tokyo 182, Japan
and
Shigeru Obayashi§ and Kazuhiro Nakahashi¶
Tohoku University, Sendai 980-8579, Japan

Introduction

THE next-generation supersonic transport (SST) is under consideration today because the Concorde has been in service for 20 years and is not fully successful economically. There are many ongoing researches in this field in the United States, Europe, and Japan. To guarantee its economic success, the next-generation SST is required to have higher lift-to-drag ratio than that of the Concorde. To achieve this goal, development of a new design technique for supersonic wings is of great interest. For the transonic wing design, Takanashi[1] proposed an inverse method that uses the "residual-correction" concept and has shown successful design results.[2] In this Note, this inverse method is extended to the supersonic wing design.

In the supersonic flow, the governing equation can be linearized. Therefore, the integration becomes simpler than that of the transonic case, but the integration region must be selected carefully because the region contributing to the point on the wing surface is limited to the Mach forecone. Sample results of two-dimensional airfoil designs confirm the validity of the present method.

Design Procedure

The inverse design method seeks a geometry that materializes the specified pressure distribution. With this target pressure distribution specified, the corresponding geometry can be obtained as follows. First, the performance of the initial geometry is analyzed by the Euler/Navier–Stokes code, and the difference between this computed pressure distribution and the target pressure distribution is calculated. If two pressure distributions coincide with each other, the initial geometry is the final geometry. If not, a geometry correction is executed by using the solution of the inverse linearized small perturbation equation. For this new geometry, the performance is analyzed and the difference from two pressure distributions is calculated. This process is repeated until the difference of pressure distributions is eliminated. Through this process, the geometry corresponding to the prescribed pressure distribution can be obtained. Figure 1 shows the flowchart of the preceding procedure.

Received May 18, 1997; revision received Sept. 28, 1998; accepted for publication Jan. 26, 1999.

*Graduate Student, Department of Aeronautics and Space Engineering.

†Research Scientist, Supercomputer Systems Engineering Division. Member AIAA.

‡Head of Applied Mathematics Laboratory, Computer Science Division. Member AIAA.

§Associate Professor, Department of Aeronautics and Space Engineering. Senior Member AIAA.

¶Professor, Department of Aeronautics and Space Engineering. Associate Fellow AIAA.

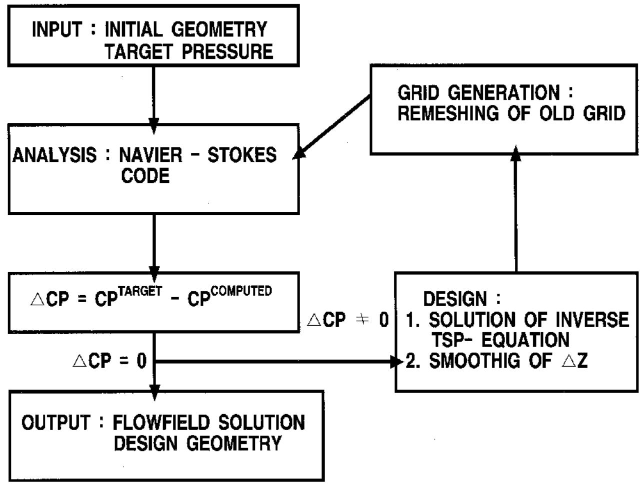

Fig. 1 Flowchart of inverse design procedure.

Integral Formulation for Inverse Method

In a supersonic flow, the small perturbation potential equation can be written in the linearized form as

$$\left(M_\infty^2 - 1\right)\bar{\phi}_{\bar{x}\bar{x}} - \bar{\phi}_{\bar{y}\bar{y}} - \bar{\phi}_{\bar{z}\bar{z}} = 0 \tag{1}$$

and pressure coefficients on wing surfaces and the tangency conditions can be written as

$$C_{p\pm}(\bar{x}, \bar{y}) = -2\bar{\phi}_{\bar{x}}(\bar{x}, \bar{y}, \pm 0) \tag{2}$$

$$\frac{\partial \bar{z}_\pm(\bar{x}, \bar{y})}{\partial \bar{x}} = \bar{\phi}_{\bar{z}}(\bar{x}, \bar{y}, \pm 0) \tag{3}$$

where the subscript "±" denotes the upper and lower surfaces of the wing. For the convenience of the computation, a Prandtl–Glauert transformation is used in the preceding equations as

$$x = \bar{x}, \qquad y = \beta\bar{y}, \qquad z = \beta\bar{z}$$
$$\phi(x, y, z) = (1/\beta^2)\bar{\phi}(\bar{x}, \bar{y}, \bar{z}) \tag{4}$$

where

$$\beta = \sqrt{M_\infty^2 - 1} \tag{5}$$

The transformed equations are written as

$$\phi_{xx} - \phi_{yy} - \phi_{zz} = 0 \tag{6}$$

$$C_{p\pm}[x, (y/\beta)] = -2\beta^2\phi_x(x, y, \pm 0) \tag{7}$$

$$\frac{\partial z_\pm(x, y)}{\partial x} = \beta^3\phi_z(x, y, \pm 0) \tag{8}$$

Assume the solution of Eq. (6) for the initial geometry $z_\pm(x, y)$ is given as $\phi(x, y, z)$. The perturbation solution $\phi(x, y, z) + \Delta\phi(x, y, z)$ should satisfy

$$(\phi_{xx} + \Delta\phi_{xx}) - (\phi_{yy} + \Delta\phi_{yy}) - (\phi_{zz} + \Delta\phi_{zz}) = 0 \tag{9}$$

$$C_{p\pm}[x, (y/\beta)] + \Delta C_{p\pm}[x, (y/\beta)]$$
$$= -2\beta^2[\phi_x(x, y, \pm 0) + \Delta\phi_x(x, y, \pm 0)] \tag{10}$$

$$\frac{\partial z_\pm(x, y)}{\partial x} + \frac{\partial \Delta z_\pm(x, y)}{\partial x} = \beta^3[\phi_z(x, y, \pm 0) + \Delta\phi_z(x, y, \pm 0)] \tag{11}$$

By subtracting Eqs. (6–8) from Eqs. (9–11), the perturbation equations are obtained as

$$\Delta\phi_{xx} - \Delta\phi_{yy} - \Delta\phi_{zz} = 0 \qquad (12)$$

$$\Delta C_{p\pm}[x, (y/\beta)] = -2\beta^2 \Delta\phi_x(x, y, \pm 0) \qquad (13)$$

$$\frac{\partial \Delta z_\pm(x, y)}{\partial x} = \beta^3 \Delta\phi_z(x, y, \pm 0) \qquad (14)$$

The solution of Eq. (12), $\Delta\phi$, can be derived by means of Green's theorem[3,4]:

$$\Delta\phi(x, y, z) = -\frac{1}{2\pi}\frac{\partial}{\partial x}\int\int_{\tau_1}\{[\Delta\phi_\zeta(\xi, \eta, +0) - \Delta\phi_\zeta(\xi, \eta, -0)]\varphi(x, y, z, \xi, \eta, 0)\}\,\mathrm{d}\xi\,\mathrm{d}\eta + \frac{1}{2\pi}\frac{\partial}{\partial x}\int\int_{\tau_1}\{[\Delta\phi(\xi, \eta, +0) - \Delta\phi(\xi, \eta, -0)] \times \varphi_\zeta(x, y, z, \xi, \eta, 0)\}\,\mathrm{d}\xi\,\mathrm{d}\eta \qquad (15)$$

where

$$\varphi(x, y, z, \xi, \eta, \zeta) = \operatorname{arc\,cosh}\frac{x-\xi}{\sqrt{(y-\eta)^2-(z-\zeta)^2}} \qquad (16)$$

The area τ_1 is that part of the $z = 0$ plane contained within the Mach forecone from the point (x, y, z); i.e., the area bounded by the line $\xi = -\infty$ and the hyperbola $(x-\xi)^2 - (y-\eta)^2 - (z-\zeta)^2 = 0$.

Because Eq. (15) includes improper integrals, the differentiation cannot move through the integral signs. This obstacle can be eliminated by using Hadamard's "finite part".[5] To utilize the pressure distributions as a boundary condition, Eq. (15) is differentiated with respect to x, and by adding the values of the resulting $\Delta\phi_x(x, y, z)$ at $z = +0$ and -0, we obtain

$$\Delta u_s(x, y) = -\Delta w_s(x, y) + \frac{1}{\pi}\int\int_{\tau_1}\frac{(x-\xi)\Delta w_s(\xi, \eta)}{\sqrt{(x-\xi)^2-(y-\eta)^2}^{\,3}}\,\mathrm{d}\xi\,\mathrm{d}\eta \qquad (17)$$

$$\Delta u_s(x, y) = \Delta\phi_x(x, y, +0) + \Delta\phi_x(x, y, -0) \qquad (18)$$

$$\Delta w_s(x, y) = \Delta\phi_z(x, y, +0) - \Delta\phi_z(x, y, -0) \qquad (19)$$

Similarly, differentiating both sides of Eq. (15) with respect to z and adding the values of the resulting $\Delta\phi_z(x, y, z)$ at $z = +0$ and -0

$$\Delta w_a = -\Delta u_a(x, y) + \frac{1}{\pi}\int\int_{\tau_1}\frac{(x-\xi)\Delta u_a(x, y)}{(y-\eta)^2\sqrt{(x-\xi)^2-(y-\eta)^2}}\,\mathrm{d}\xi\,\mathrm{d}\eta \qquad (20)$$

$$\Delta u_a(x, y) = \Delta\phi_x(x, y, +0) - \Delta\phi_x(x, y, -0) \qquad (21)$$

$$\Delta w_a(x, y) = \Delta\phi_z(x, y, +0) + \Delta\phi_z(x, y, -0) \qquad (22)$$

By solving Eqs. (17) and (20) with the boundary conditions Δu_s and Δu_a, the geometry terms Δw_s and Δw_a can be obtained. As defined in Eqs. (19) and (22), $\Delta w_s(x, y)$ and $\Delta w_a(x, y)$ represent the derivatives of thickness and camber correction, respectively.[6] Therefore, the value of geometry correction can be computed by performing the numerical integration in the x direction:

$$\Delta z_\pm(x, y) = \frac{1}{2}\int_{\mathrm{LE}}^{x}\Delta w_a(\xi, y)\,\mathrm{d}\xi \pm \frac{1}{2}\int_{\mathrm{LE}}^{x}\Delta w_s(\xi, y)\,\mathrm{d}\xi \qquad (23)$$

Results

To confirm the validity of the present formulation of the inverse method for the supersonic wing design, numerical calculations are performed in two dimensions. A Navier–Stokes code is used as an analysis code. This code utilizes a total variation diminishing upwind scheme for the spatial discretization of the convective terms and the lower-upper, symmetric Guass–Seidel method for the time integration. The computational grid is generated by an algebraic grid generation code.

NACA 1204 and NACA 0003 are selected as reference airfoils. First, the NACA 1204 airfoil is designated as a target airfoil. By taking its pressure distribution as a target, the present inverse design code is applied to reconstruct its shape, starting from the NACA 0003 airfoil. The flow condition is assumed as $M_\infty = 2.0$, $Re = 1.45 \times 10^7$, and $\alpha = 0$ deg. The design result is shown in Fig. 2. Both target and computed geometries and pressure distributions coincide with each other.

NACA 66003 is selected as a reference airfoil for the second test case. First, pressure distributions of this airfoil are calculated at both 0- and 2-deg angles of attack, and the pressure distribution at 2-deg angle of attack is designated as a target. The design procedure starts with the pressure distribution over the NACA 66003 airfoil at 0-deg angle of attack.

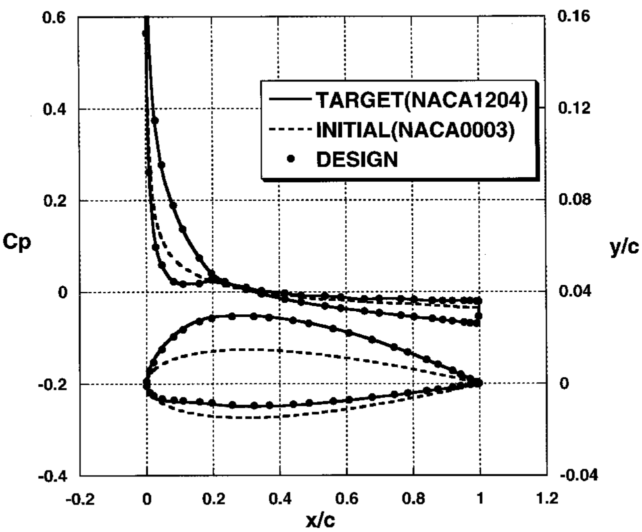

Fig. 2 Inverse design result and comparison of pressure distributions to reconstruct the NACA 1204 airfoil.

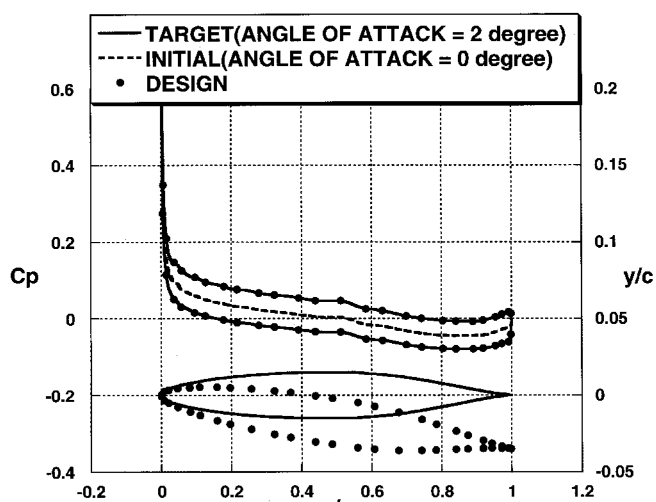

Fig. 3 Inverse design result and comparison of pressure distributions to reproduce the specified angle of attack.

As shown in Fig. 3, the designed airfoil inclined 2 deg as specified in the target pressure distribution.

Conclusions

In this investigation, Takanashi's inverse design method is extended to supersonic airfoil design. Numerical results show that the present inverse code can be used to change not only geometries but also the angle of attack of airfoils. The extension to three dimensions is straightforward because the present formulation is derived in the three-dimensional form.

When using the inverse method as a design tool, designers must translate their design criteria of supersonic wings into target pressure distributions. The determination of optimal target pressure distributions will be studied in the future.

References

[1]Takanashi, S., "Iterative Three-Dimensional Transonic Wing Design Using Integral Equations," *Journal of Aircraft*, Vol. 22, No. 8, 1985, pp. 655–660.

[2]Obayashi, S., Jeong, S. K., and Matsuo, Y., "New Blunt Trailing-Edge Airfoil Designed by Inverse Optimization Method," *Journal of Aircraft*, Vol. 34, No. 2, 1997, pp. 255–257.

[3]Lomax, H., Heaslet, M. A., and Fuller, F. B., "Integrals and Integral Equation in Linearized Wing Theory," NACA 1054, 1951.

[4]Heaslet, M. A., Lomax, H., and Jones, A. L., "Volterra's Solution of the Wave Equation as Applied to Three-Dimensional Supersonic Airfoil Problem," NACA 889, 1947.

[5]Hadamard, J., "Lectures on Cauchy's Problem in Linear Partial Differential Equations," Yale Univ. Press, New Haven, CT, 1928.

[6]Carlson, H. W., and Middleton, W. D., "A Numerical Method for Design of Camber Surfaces of Supersonic Wings with Arbitrary Planforms," NASA TN D-2341, 1964.

New Technique for Preventing Payload-Airbag Overtipping

Zhimin Xie,* Zhimin Wan,† and Xingwen Du‡
Harbin Institute of Technology,
Harbin 150001, People's Republic of China

Nomenclature

F = retarding force, N
F_m = maximum retarding force, N
h = stroke, m
h_e = height of airbag, m

Introduction

AIRBAGS have increased in popularity for the impact attenuation of target, reconnaissance drones, and training missiles, as well as for the landing of aircrew escape modules.[1] The airbag technique has many advantages such as high energy absorption capability and good adaptability to landing surface conditions. Because of the existence of the airbags, however, the c.g. of the recovery system will be raised, which leads to low stability and more chance of tipover. The stability of airbags in windy landings or when suspended from an oscillating parachute is a problem. For example, the encapsulated seat bags used on the B-70 were unsatisfactory in a side-wind landing because of the poor relationships between the bag diameter and the vehicle. To improve stability, two sausage-shaped airbags were used on the Matador/Mace,[1,2] whereas several bags were mounted on the F-111 and B-1 crew modules.[1] These airbags have pressure-relief valves. In some cases, gas-relief valves are not considered. An example of this application is in the Pathfinder mission, where the spherical airbags were designed to protect the lander from impacting with the Martian surface.[3]

In this work a new multicompartment structure design technique that prevents the payload-airbag recovery system from tipover is presented. The airbag with a constant venting area, divided into several compartments by internal membranes with several linking holes, is distinguished in function from the dual-compartment structure bags used on the BQM-34V.[1] By controlling the gas flowing rate to get different stiffnesses in different parts of the bag at ground contact, the payload can drop steadily on the bags. Using a special internally designed structure, the present bags can provide better protection than the single-compartment bag.[2,4] Experiments on the simulated model–airbag system show that the new technique is effective in stopping the payload from tipover.

Multicompartment Airbag

For the purpose of increasing the landing stability and preventing a payload–airbag system tipover, several compartments are considered in the internal structure of the airbag. The number of compartments depends on the attenuation requirement. Two kinds of airbags were designed for the simulated missile and capsule, respectively.

Consider that the recovery payload is a training missile and that the airbag has a cube-like form divided into three compartments connected to each other by the linking holes at the membranes. The sketch of the missile–airbag system is shown in Fig. 1a. At a predetermined level, pressure-relief valves open and allow the gas of the center compartment to escape. At the same time, the gas of the two side compartments passes the holes into the center part and then flows out. The flowing rate depends mostly on the linking hole's dimension, and so by adjusting the hole's dimension, the side parts have a greater stiffness than the center part. Support from the side parts restrains the missile on the center of the bags, and tipover is avoided. Another kind of airbag is used for the landing attenuation of a conic capsule (Fig. 1b). It has a circular shape and is divided into two compartments by means of a cylindrical membrane with several linking holes. During the landing impact, the open orifices allow the gas of the inner compartment to blow out and the gas of the outer compartment then flows out of the airbag. This results in a higher instantaneous stiffness in the outer compartment than that in the inner one, which contributes notably to the stability of the landing capsule.

Experiments and Results

The cube- and circular-formed airbags used for the simulated missile and capsule were investigated, respectively. Because of the siender characteristic of the missile, a cluster of bags consisting of two cube-shaped and two cylindrical bags were fabricated. The

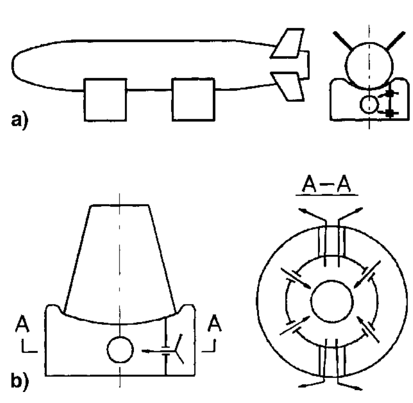

Fig. 1 Sketch of payload–airbag systems.

Received Nov. 24, 1997; revision received June 20, 1998; accepted for publication July 15, 1998.

*Graduate Student Research Laboratory of Composite Materials, School of Astronautics.

†Associate Professor, Analysis and Measurement Center.

‡Professor, Research Laboratory of Composite Materials, School of Astronautics.